Est. 1984

ORIENTAL JOURNAL OF CHEMISTRY
An International Open Access, Peer Reviewed Research Journal

www.orientjchem.org

ISSN: 0970-020 X
CODEN: OJCHEG
2022, Vol. 38, No.(1):
Pg. 172-176

Fabrication of MnO_2 Nanoparticles from Simple Pyrolytic Method for Degradation of Methylene Blue Under Visible Light Irradiation

SANDIP MONDAL

Department of Chemistry, Suri Vidyasagar College, Suri, West Bengal-731101, India.
*Corresponding author E-mail: mondalsandip10@gmail.com

http://dx.doi.org/10.13005/ojc/380121

(Received: October 25, 2021; Accepted: January 20, 2022)

ABSTRACT

α-MnO_2 nanoparticle with semi-tubular morphology was prepared pyrolytically using $[Mn(pyo)_2(dca)_2]_n$ as a sole precursor at 700^{O}C in air for 2 h without applying any catalyst or template. This nanostructure was systematically characterized physically by Fourier transform infrared (FT-IR) spectroscopy, X-ray diffraction spectroscopy (XRD), scanning electron microscopy (SEM) and thermal gravimetric analysis (TGA). The prepared α-MnO_2 displayed high photocatalytic activity toward decolorization of methylene blue (MB) dye under visible light irradiation in assistance with H_2O_2. The result obtained indicated that almost 84% colour removal occured within 2.40 h.

Keywords: Manganese oxide, Nanoparticles, Pyrolytic technique, Photocatalytic activity.

INTRODUCTION

Most of the wastewater of textile industries contains large quantities of azo compounds. Discharge of such harmful chemicals may contaminate into our surface water and cause serious water pollution.[1] The consequence of such environmental carcinogens in defiled water has been extensively studied.[2] Considerable research efforts were carried out to remove the colour of untreated effluents from textile industries. These include several chemical, physical as well as biological methods, such as chemical coagulation [3], anaerobic and aerobic[4], microbial degradation[5], use of activated carbon[6], biosorption[7], chemical oxidation[8], deep-well injection, incineration, solvent extraction and irradiation[9–12] etc. Among the several elegant techniques, Advanced Oxidation Process (AOP) is the most promising advancement *via* the generation of highly active radicals which are very effective for oxidizing most hazardous organic compounds into harmless products.[13,14] Catalytic oxidation process has emerged as one of the most efficient methods as it involves effective mineralization of organic substances.[15]

Manganese oxides nanomaterials attracted much attention due to markedly increased surface area as a consequence of greatly decreasing size.[16,17] These nanomaterials show wide application in various fields, especially, wastewater treatment, catalysis, biosensors, ion-exchange, molecular

adsorption, energy storage devices (rechargeable batteries, supercapcitors), imaging, and so on.[18-21] Interestingly, MnO_2 catalysts offer substantial activity towards oxidation-reduction reactions. However, there are only a few studies have demonstrated the degradation of methylene blue from wastewater by using MnO_2 nanocrystals as photocatalyst.[22-24]

Several different strategies have been employed to fabricate MnO_2 nanoparticles with various morphologies over the last few years.[25-27] However, coordination polymers are interesting for several reasons but their use as precursors for the preparation of nano-scale-materials has not been yet investigated in details. This paper describes the utilization of a coordination polymer, $[Mn(pyo)_2(dca)_2]_n$ as the only precursor to synthesize α-MnO_2 nanoparticle by simple pyrolytic technique without using any catalyst or template and photocatalytic activity for the degradation of methylene blue has been investigated in assistance with H_2O_2 as co-catalyst. Additionally, hydroxyl radical mechanism for colour removal of methylene blue was investigated.

EXPERIMENTAL

Materials and Physical Methods

Pyridine-N-oxide was purchased from Alfa Aesar, sodium dicyanamide from Fluka, Manganese (II) Chloride from Aldrich Chemical Company Inc. and Methylene blue was obtained from Merck & Co., Inc. All chemicals were of analytical grade and used without any further purification. The crystal phase of the synthesized sample was examined using powder X-ray Diffractometer with Cu–Kα radiation [Philips (PANalytical), Model: PW1830]. The Scanning electron microscopy (Hitachi S-3400N) was used to determine the morphology of the nanostructure. FT-IR spectrum was performed on Perkin-Elmer RXI FTIR spectrophotometer using KBr disks (400-4000 cm^{-1}). The UV-Vis spectrophotometric measurements were carried out using a U-3501 HITACHI, Japan over the wavelength range of 400 to 800nm for investigating the photocatalytic study. A thermal analysis (TG–DTA) was taken with a TGA/SDTA851^e Metler-Toledo thermal analyzer.

Photocatalytic studies

The photocatalytic activity of the synthesized nanoparticle was investigated by photo-degradation of methylene blue aqueous solution. The photocatalytic degradation experiments were performed in a 100 mL capacity glass reactor with exposure of light. 50 mL aqueous solution of methylene blue (2×10^{-6} M), 200 μL 30% solution of H_2O_2 and 4 mg of MnO_2 nanoparticles were mixed by maintaining constant mechanical stirring. At specific time intervals, 5 mL sample was withdrawn and centrifuged to separate the catalyst. The progress of the decolorization process was followed by monitoring the decrease in intensity at λ_{max}, *i.e.,* 663nm of the dye solution.

Syntheses of α-MnO_2 nanoparticale

The complex $[Mn(pyo)_2(dca)_2]_n$ was synthesized and characterized by the procedure reported earlier.[28] The pure prepared $[Mn(pyo)_2(dca)_2]_n$ complex was taken in a platinum crucible and calcined in air maintaining 700°C temperature for 2 h to get nano-sized MnO_2 inside platinum-crucible after oxidation. The prepared α-MnO_2 was washed thoroughly with ethanol followed by water, and then dried at 50°C for 6 hours.

RESULTS AND DISCUSSION

To obtain appropriate calcination temperature, thermo-gravimetric analysis of the complex, $[Mn(pyo)_2(dca)_2]_n$ was carried out (SI File). On further heating weight loss of the sample occurs accordingly, but around 700°C, there was no change in sample weight indicating the production of pure inorganic oxides. The FT-IR spectra of synthesized MnO_2 (SI File) indicate the band exhibited in the range 400-800 cm^{-1} which was assigned to Mn-O lattice vibration.[29] The XRD patterns of the synthesized MnO_2 are shown in Fig. 1a. All the visible peaks indexed to α-MnO_2 (JCPDS, file No. 44-0141)[30]. The average grains size was determined by using the Scherrer equation,

$$d = \frac{k\lambda}{\beta_s \cos\theta}$$

Where *d* is the mean size of the crystallite grains, k is a dimensionless shape factor whose value close to unity (0.9), λ is the wavelength of Cu-Kα radiation, β_s is the line broadening at half the maximum intensity (FWHM) of the diffracted peak of sample and is given by $\sqrt{\beta_{Ex}^2 - \beta_{Ins}^2}$, θ is the Bragg angle. The morphology of the synthesized MnO_2 was

characterized by FE-SEM (Fig. 1b) which consists of semi-tubular structure.[31] The SEM image was also used to obtain the particle size of the synthesized sample. The particle size obtained from the SEM image was in well agreement with that calculated from the XRD data. The estimated particle size of MnO_2 was found to be ~75nm.

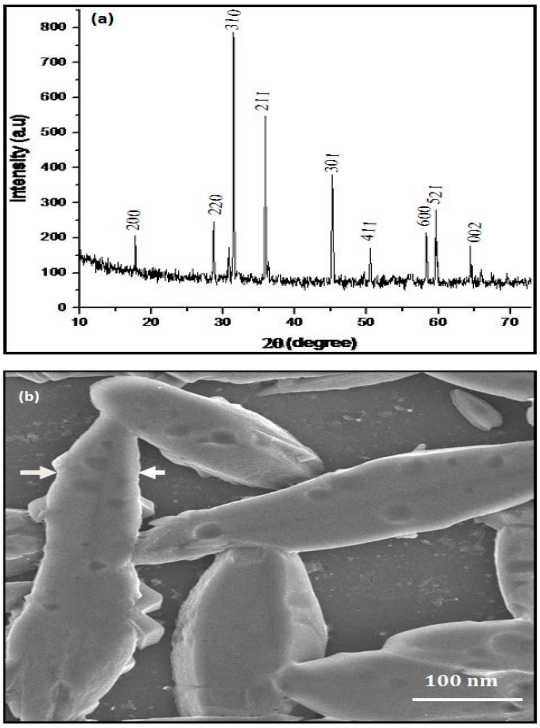

Fig. 1(a) Powder XRD pattern and (b) FE-SEM image for MnO_2 nanoparticles

The photocatalytic activity investigation experiment of the synthesized product was determined by photo-degradation of methylene blue in aqueous solution in presence and as well as absence of that catalyst in assistance with hydrogen peroxide under visible light irradiation for 160 min (Fig. 2). It was observed that, during the experiment, assistance of H_2O_2 may play a vital role as it increases the catalytic activity of MnO_2 nanoparticles. This is because of generation of highly active hydroxyl radical (•OH) during photocatalysis process having higher oxidizing properties in comparison with H_2O_2.

In presence of the MnO_2 photocatalysts about 84% colour removal was observed in 2 h 40 min, though only 6% colour removal was detected in absence of catalyst (Figure 3).

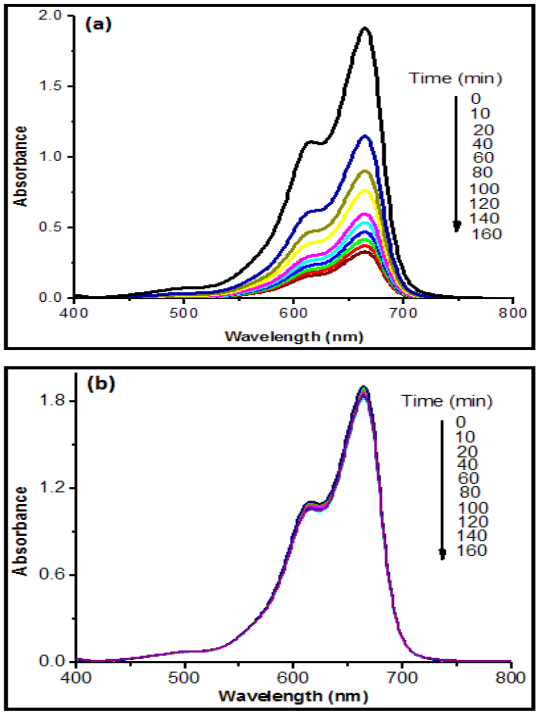

Fig. 2(a). Adsorption intensity for methylene blue in presence of α-MnO_2 as the catalyst performed in assistance of H_2O_2. (b) Corresponding adsorption intensity in absence of the above catalyst

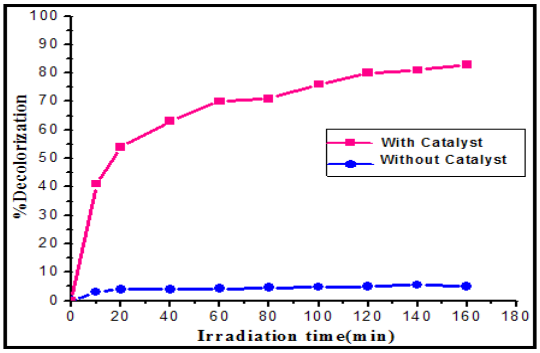

Fig. 3. Comparison of the degradation percentage changes of methylene blue with times in presence and absence of the catalyst

However, no characteristic degradation of MB was observed with only H_2O_2. The kinetic study reveals that the photodegradation of MB follows pseudo-first-order kinetics with the concentration of MB (Figure 4).

This relation can be described as:

$$\ln\left(\frac{C_0}{C}\right) = K_a t$$

Where C_0 is the initial concentration when irradiation starts (t=0) and K_a is the photodegradation rate constant calculated from the slope of $\ln(C_0/C)$ vs. t ((minutes). From the plots, the calculated K_a value was found about 1.28×10^{-2} minute^{-1}.

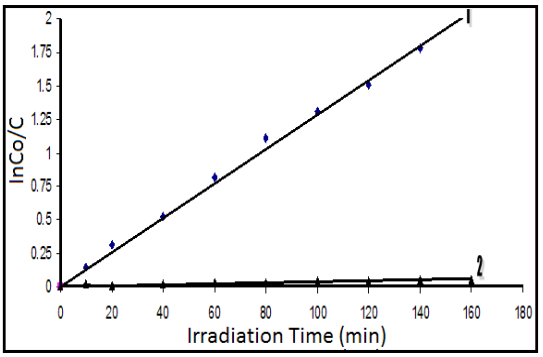

Fig. 4. Degradation kinetics of methylene blue vs. irradiation time: (1) in presence of the catalyst and (2) in absence of the catalyst

The increase of catalytic activity in presence of H_2O_2 was ascribed to the involvement of considerable numbers of hydroxyl radical. A possible mechanism for the degradation methylene blue catalyzed by MnO_2 nanoparticle is supposed.[32]

$MnO_2 + h\nu \rightarrow MnO_2 (e_{CB}^- + h_{VB}^+)$
$MnO_2 (h_{VB}^+) + H_2O \rightarrow MnO_2 + H^+ + {}^{\cdot}OH$
$MnO_2 (e_{CB}^-) + H_2O_2 \rightarrow MnO_2 + OH^- + {}^{\cdot}OH$
${}^{\cdot}OH + MB \rightarrow$ degradation products

Actually, during the photocatalytic process, when a semiconductor material like MnO_2 nanoparticles having indirect band gap of 1.3 eV, which exhibits ~1 eV blue shift from that of the bulk MnO_2 materials[33] are irradiated with photon, electrons excited from the valence to conduction band and generate holes (h_{VB}^+) in valence band. Those photo generated holes, h_{VB}^+, can react with water species, which are absorbed on the surface of MnO_2, to generate the hydroxyl radical. However, the formation of the OH radicals occurs only when visible light irradiation and hydrogen peroxide (H_2O_2) both are present in semiconductor-based photocatalytic reaction. An interaction between the electrons of conduction band of MnO_2 and H_2O_2 under visible light irradiation can accelerate the production of a large number of hydroxyl radicals. The generation of active •OH radicals ($E^0 = 2.85V$) by the decomposition of H_2O_2 can initiate photocatalytic degradation of organic dyes.[34] However, the inability of •OH radicals formation from the direct dissociation of H_2O_2 was observed because it cannot absorb visible light. In photochemical reaction the rate of catalytic activity depends on the concentration of hydroxyl radical. However, it is worth mentioning that degradation rate increases with increasing H_2O_2 concentration up to a threshold. As the optimum point reached, further addition of H_2O_2 can decrease the degradation rate due to the fact that H_2O_2 itself is a scavenger[35] of •OH accordance with the reaction below:

$$\bullet OH + H_2O_2 \rightarrow \bullet OH_2 + H_2O$$

CONCLUSION

In summary, α-MnO_2 nanoparticle was prepared pyrolytically employing coordination polymers $[Mn(pyo)_2(dca)_2]_n$ as a sole precursors. Particle size and morphology of the synthesized MnO_2 nanoparticle have been studied by physicochemical techniques. Such nanomaterial exhibited a very good performance in the decolorization of methylene blue under visible light irradiation in assistance with H_2O_2. It displayed ~ 84%, degradation of MB within 2 h 40 minute. In absence of the catalyst 6% degradation of dye was detected only.

ACKNOWLEDGMENT

The author sincerely acknowledges the Department of Polymer Science, University of Calcutta, West Bengal for providing necessary instrumental facilities for completion of the work.

Conflict of interest

The author declares that there is no conflict of interest.

REFERENCES

1. Lellis, B.; Fávaro-Polonio, C. Z.; Pamphile, J. A.; Polonio, J. C. *Biotechnology Research and Innovation.*, **2019**, *3*, 275-290.
2. Rauf, M. A.; Ashraf, S. S. *J. Hazard. Mater.*, **2009**, *166*, 6-16.
3. Rodriguesa, C. S. D.; Madeira, L. M.; Boaventura, R. A. R. *Environ. Technol.*, **2013**, *34*, 719–729.
4. Yurtsever, A.; Sahinkaya, E.; Aktaş, Ö.; Uçar, D.; Ç ınar, Ö.; Wang, Z. *Bioresour. Technol.*, **2015**, *192*, 564-573

5. Varjani, S.; Rakholiya, P.; Yong Ng, H.; You, S.; Teixeira, J. A. *Bioresour. Technol.*, **2020**, *314*, 123728.
6. Wong, S.; Yac'cob, N. A. N.; Ngadi, N.; Hassan, O.; Inuwa, I. M. *Chinese J. Chem. Eng.*, **2018**, *26*, 870-878.
7. Kabbout, R.; Taha, S. *Physics Procedia.,* **2014**, *55*, 437-444.
8. Donkadokula, N. Y.; Kola, A. K.; Naz, I.; Saroj, D. *Rev. Environ. Sci. Biotechnol.*, **2020**, *19*, 543–560.
9. Abdelkreem, M.; *APCBEE Procedia.*, **2013**, *5*, 349-357.
10. Vergili, I.; Kaya, Y.; Sen, U.; Gönder, Z. B.; Aydiner, C. *Resour. Conserv. Recy.*, **2012**, *58*, 25–35.
11. Borges, G. A.; Silva, L. P.; Penido, J. A.; de Lemos, L. R.; Mageste, A. B.; Rodrigues, G. D. *J. Environ. Manag.*, **2016**, *183*, 196-203.
12. He, S.; Sun, W.; Wang, J.; Chen, L.; Zhang, Y.; Yu, *J. Radiat. Phys. Chem.*, **2016**, *124*, 203-207.
13. Badmus, K. O.; Tijani, J. O.; Massima, E.; Petri, L. *Environ. Sci. Pollut. Res.*, **2018**, *25*, 7299–7314.
14. Tijani, J. O.; Fatoba, O. O.; Madzivire, G.; Petrik, L. F. *Water Air Soil Pollut.*, **2014**, *225*, 2102-2130.
15. Luo, X.; Liang, H.; Qu, F.; Ding, A.; Cheng, X.; Tang, C. Y.; Li, G. *Chemosphere.*, **2018**. *200*, 237-24.
16. Xu, B.; Lu, H.; Cai, W.; Cao, Y.; Deng, Y.; Yang, W. *Electrochimica Acta.*, **2019**, *305*, 360-369.
17. Khandare, L.; Terdale, S.; *Appl. Surf. Sci.,* **2016,** *418*, 22-29.
18. Cao, J.; Mao, Q. H.; Shi, L.; Qian, Y. T. *J. Mater. Chem.*, **2011**, *21*, 16210-16215.
19. Yamaguchi, Y.; Aono, R.; Hayashi, E.; Kamata, K.; Hara, M. *Appl. Mater. Interfaces.*, **2020**, *12*, 36004–36013.
20. Zhou, M.; Zhang, X.; Wei, J.; Zhao, S.; Wang, L.; Feng, B. *J. Phys. Chem. C.*, **2011**, *115*, 1398–1402
21. Cao, Z.; Yang, Y.; Qin, J.; Su, Z. *J. Power Sources.*, **2021**, *491*, 229577.
22. He, Y.; Jiang, D. B.; Chen, J.; Jiang, D. Y.; Zhang, Y. X. *J. Colloid Interface Sci.,* **2018**, *510*, 207–220.
23. Bao, X.; Qin, Z.; Zhou, T.; Deng, J. *J. Environ. Sci.*, **2018**, *65*, 236-245.
24. Zhang, Y. X.; Hao, X. D.; Li, F.; Diao, Z. P.; Guo, Z. Y.; Li, *J. Ind. Eng. Chem. Res.*, **2014**, *53*, 6966–6977.
25. Kumar, A.; Sanger, A.; Kumar, A.; Kumar, Y.; Chandra, R. *Electrochimica Acta.*, **2016**, *220*, 712-720.
26. Ding, B.; Zheng, P.; Ma, P.; Lin, *J. Adv. Mater.,* **2020**, *19,* 05823.
27. Liu, X.; Chen, C.; Zhao, Y.; Jia, B. *Journal of Nanomaterials,* Special Issue., **2013**, Article ID 736375, 1-7.
28. Mondal, S.; Guha, A.; Suresh, E.; Jana, A. D.; Banerjee, A. *J. Mol. Str.*, **2012**, *1029*, 169-174.
29. Kanga, L.; Zhang, M.; Liu, Z.-H. *Spectrochimica Acta Part A.*, **2007**, *67*, 864-869.
30. Feng, L; Xuan, Z; Zhao, H; Bai, Y; Guo, J; Su, C; Chen, X. *Nanoscale Res. Lett.*, **2014**, *9*, 290.
31. Zhang, Y.; Wang, W.; An, Y.; Zhang, F.; Yin, Y.; Dong, L. *Mater. Lett.*, **2012**, *69*, 7-9.
32. Osgouei, M.S.; Khatamian, M.; Kakili; H. *Mater. Chem. Phy.*, **2020**, *239*, 122108.
33. Gao, T.; Glerup, M.; Krumeich, F.; Nesper, R.; Fjellvåg, H.; Norby, P. *J. Phys. Chem. A.*, **2008**, *112*, 13134–13140.
34. Tang, Y.C.; Huang, X.H.; Yu, H.Q.; Li, W.H.; Wu, C.N. *Adv. Mater. Res. Trans. Tech. Publ.,* **2011**, *287-290*, 1612-1619.
35. Chandra, S.; Das, P.; Bag, S.; Bhar, R.; Pramanik, P. *Mater. Sci. Engin.* B., **2012**, *177*, 855-861.